Sustainable β-Cyclodextrin/Polyethylenimine-Encapsulated Activated Algae Hydrogel Beads for High-Capacity Cd(II) Removal: Adsorption Performance, Mechanism, Thermodynamics, and Box–Behnken Optimization

Table S1. Chemical name, formula, and company.

Chemical name	**Formula**	**Company**
Polyethylenimine	$C_{24}H_{63}N_{13}$	Sigma-Aldrich, Germany
β-Cyclodextrin	$C_{42}H_{70}O_{35}$	Sinopharm Chemical Reagent Co., Ltd, China
Epichlorohydrin, 99%	C_3H_5ClO	Thermoscientafic
Algae		Beach of mediterinane sea
Cadmium acetate	$Cd(CH_3CO_2)_2(H_2O)_2$	Sigma-Aldrich, Germany
Sodium hydroxide	NaOH	LOBA CHEMIE PVT.LTD, India
Hydrochloric acid 37%	HCl	LOBA CHEMIE PVT.LTD, India
Ethanol	C_2H_5OH	LOBA CHEMIE PVT.LTD, India
Methanol	CH_3OH	LOBA CHEMIE PVT.LTD, India

Table S2. Instruments and equibments.

Test name	Abbrevation	Instrument name	Company	Illustration
Fourier transformer infrared	FT-IR	A Nicolet IS10 Fourier transform infrared (FTIR) spectrometer	Thermo Fisher Scientific, Waltham, MA, USA	equipped with an attenuated total reflectance accessory and which ran in the 4000-400 cm^{-1} range was used to gather FTIR spectra
Powered X-ray diffraction	PXRD	Siemens diffractometer (model D500, Germany)	Germany	patterns were captured from powder samples through the use of a Siemens diffractometer (model D500, Germany) that was fitted with a Cu-K radiation source (wavelength 1.54 Angstroms (Å)) operating at 30 kV and 20 mA.
Scanning Electron Microscope	SEM	(JSM-6510LV, JEOL Ltd., Tokyo, Japan)	JEOL Ltd., Tokyo, Japan	The morphology of the investigated sorbents was analyzed with the use of a scanning electron microscope
X-ray photoelectron spectroscopy	XPS	K-ALPHA (Themo Fisher Scientific, USA)	Themo Fisher Scientific, USA	Used for determination the elemental analysis for the compound
Braunnar Emmet Teller	BET	Quantachrome Instruments, Anton Paar Quanta Tec, Inc., Boynton Beach, FL,	Quanta Tec, Inc., Boynton Beach, FL, USA	was utilised for surface and pore analysis (Brunauer Emmett-Teller (BET) surface area, porous volume, and pore size), and NovaWin Software (v11.0) was used for data interpretation.

		USA		The BET surface area of material adsorbents was obtained by the application of nitrogen adsorption-desorption isotherms at 77K through the use of a specific analyser (Quadrasorb–EVO, Quantachrome, USA).
Atomic adsorption spectrometer		PerkinElmer atomic absorption spectrometer (PinAAcle 500), Singapore	PerkinElmer, Singapore	Measuring the metal ion concentration.
Energy Dispersive X-ray	EDX	Leo1430VP microscope	Carl Zeiss AG, Jena, Germany	Elemntal analysis of the material
Transmission electron microscopy	TEM	TEM, FEI Teanci G2 F20, USA	FEI Teanci G2 F20, USA	Determination the morphology of the material and size
pH meter	pH	HANNA (model 211)	USA	Measuring the acidity or basicity of the solution
Sonication	Ultrasonic	Elmasonic P300H ultrasonic bath, continuous mode, power 380 W	Elma Schmidbauer GmbH, Singen, Germany	Sonication of the material as well as used ton disperse material on the solution as it decrease the particle size of the material
Water bath	Shaking	GFL Orbital Shaker 3017		

Table S3. True variables for the adsorption process factors.

Factors	pH	Time (min.)	Initial concentration (mg/L)	Temprature (^{o}C)	Dose (g)
pH	2-8	30	200	25	0.02
Dose (g)	6	30	300	25	0.02-0.5
Initial concenteration	6	100	20-380	25	0.02
Time (min.)	6	5-100	300	25-45	0.02
Temperature	6	30	300	20-45	0.02

Table S4. True variables, codes, and their BBD levels.

Code	Variables	-1	0	+1
A	pH	2	7	12
B	Dose (g)	0.02	0.26	0.5
C	Time (min.)	5	55.5	100

Table S5. Crystalographic data.

hkl	2θ Observed	2θ Calculated	Difference
-1 2 1	12.5281	12.4945	0.0336
1 1 1	17.1265	17.0705	0.056
-2 0 0	18.6877	18.6408	0.0469
-2 2 0	20.3658	20.3251	0.0407
0 5 1	22.5096	22.4675	0.0421
-1 4 2	23.5758	23.525	0.0508
-1 5 2	26.5393	26.5139	0.0254
2 3 1	28.0104	27.9779	0.0325
-3 1 0	28.454	28.4159	0.0381
-3 2 0	29.2759	29.289	-0.0131
-3 2 3	30.0752	30.0847	-0.0095

-2 6 2	31.1357	31.1023	0.0334
-3 4 0	32.5596	32.5682	-0.0086
-1 5 3	33.3631	33.3265	0.0366
-4 0 1	33.8129	33.7995	0.0134
-2 2 4	35.4326	35.4516	-0.019
-1 0 4	36.0592	36.0696	-0.0104
-3 2 4	36.4646	36.4396	0.025
-1 2 4	37.0402	37.0131	0.0271
-1 3 4	38.1712	38.1642	0.007
-4 3 0	39.8749	39.8159	0.059
1 9 1	40.5121	40.5481	-0.036
-1 5 4	41.6241	41.6666	-0.0425
3 2 2	43.0536	43.0735	-0.0199
-2 1 5	44.1067	44.1071	-0.0004
1 1 4	45.93	45.9769	-0.0469
-1 7 4	46.5032	46.5121	-0.0089
0 6 4	47.3209	47.3336	-0.0127
-5 5 1	48.2914	48.276	0.0154
-4 8 4	51.5845	51.6058	-0.0213
1 12 1	52.7499	52.7392	0.0107
2 2 4	53.6503	53.644	0.0063
-1 13 1	55.1186	55.1176	0.001
4 5 2	55.9705	55.9803	-0.0098
-6 6 4	57.4181	57.4315	-0.0134
-7 1 3	59.017	59.0423	-0.0253
-7 2 4	59.8432	59.8874	-0.0442
-7 4 2	63.0221	63.0165	0.0056
5 3 3	71.9132	71.9115	0.0017
-5 0 8	73.106	73.1115	-0.0055
-8 5 2	74.7806	74.7708	0.0098

Table S6. Equations used in this work to fit the data of adsorption experiments.

Serial	Equation	Nmae	Description	Ref.
1	$q_e = \frac{q_m}{1 + K_L C_e}$	Langmuir	q_e (mg.g^{-1}) Adsorption capacity, C_e equilibrium concentration, q_m (mg.g^{-1}) is the monolayer saturation capacity constant and K_L (L/mg) is the Langmuir constant associated with the free adsorption energy. The favorability of the adsorption process in the Langmuir model is determined by means of the R_L dimensionless factor ($R_L = 1/(1 + k_L \cdot C_0)$) as follows: $R_L = 0$, $0 < R_L < 1$, $R_L = 1$, and $R_L > 1$ indicating irreversible, favorable, linear, and unfavorable adsorption isotherms, respectively.	[1]
2	$q_e = K_F C_e^{\frac{1}{n}}$	Freundlich	K_F Freundlich isotherm constants [(mg/g)/(mg/L)$^{1/n}$], and $1/n$ represents the exponent of non-linearity (i.e., C-type, L-type, and S-type isotherms). n is the Freundlich constants, and $n < 1$ indicates poor adsorption while $n = 1$–2 and $n = 2$–10 indicate average and good adsorptions, respectively. The values of n and k_f are calculated, respectively	[2]
3	$q_e = q_m \exp(-\beta\varepsilon^2)$ $\varepsilon = RT ln\left(1 + \frac{1}{C_e}\right)$ $E_{DR} = \sqrt{\frac{1}{2K_{DR}}}$	Dubinin–Radushkevich	q_D is the maximum monolayer adsorption capacity (mg/g), B_D is the activity coefficient related to the apparent free energy of adsorbate adsorption onto the adsorbent (mol^2/kJ^2), ε_D is the Polanyi potential which is related to the equilibrium concentration, and E is the mean adsorption energy.	[3]
4	$q_e = Q_{max} \frac{RT}{b} \ln(K_T C_e)$	Temkin	K_T is the Temkin isotherm constant or equilibrium binding constant (L/mg) corresponding to the maximum binding energy, and b_T is the Temkin isotherm constant related to the heat of adsorbate adsorption onto the adsorbent due to adsorbent-adsorbate interaction (J/mol), R is the gas constant (8.314 J/mol/K), and T is the absolute temperature (herein 298 K).	[4]

5	$q_e = \frac{KC_e}{1 + JC_e^n}$	Jossens	The Jossens adsorption isotherm defines the relationship between adsorbate amount (q_e, mg g^{-1}) and its concentration (C_e, mg L^{-1}). The maximum capacity (q_m, mg g^{-1}) reflects the theoretical limit of filled sites. The affinity constant (K, L mg^{-1}) shows interaction strength; higher values mean stronger forces. The heterogeneity factor (n) indicates variance in adsorption behavior values near one suggest Langmuir behavior, while others point to heterogeneous adsorption. These parameters are typically estimated via non-linear regression of experimental data.	[5]
6	$q_t = q_e\left(1 - e^{K_1 t}\right)$	Pseudo-First-order kinetic	q_e and q_t are the adsorption capacities at equilibrium and time t (mg/g), and k_1 is the rate constant (min^{-1}), respectively.	[6]
7	$q_t = \frac{tK_2 q_e^2}{1 + q_e K_2 t}$	Pseudo-Second-order kinetic	k_2 is the pseudo-second order constant (mg/(g.min))	[7]
8	$q_t = K_i t^{1/2} + X$	Intraparticle diffusion	q_t is the adsorption capacity at time t in (mg/g), k_{int} is the intraparticle diffusion rate constant ($mg \cdot g^{-1} \cdot min^{-1/2}$), and C is a constant related to the the thickness of the boundary layer (mg/g).	[8]
9	$q_t = \frac{1}{\beta} \ln(\alpha\beta t + 1)$	Elovich	The constants α chemical adsorption rate ($mg.g^{-1}min^{-1}$), and β Coefficient in relation with extension of covered surface	[9]
10	$\Delta G^o = \Delta H^o - T\Delta S^o$	Gibbs free energy	ΔG°: Gibbs free energy change; Kd: equilibrium constant; R: gas constant; T: temperature.	[10]
11	$LnK_d = \frac{\Delta S^\circ}{R} - \frac{\Delta H^\circ}{RT}$	Van't Hoff	ΔS°: entropy change; ΔH°: enthalpy change.	[11]
12	$LnK_d = lnA - (\frac{Ea^0}{R})\frac{1}{T}$	Arhinus	Ea was the activation energy, A Arhinus constant, R ideal gas constant 8.314 J/mol K, T (K) is the absolute solution temperature	[12]

Table S7. The parameter of the adsorption isotherm for Cd(II) ions on FAACP hydrogel beads.

Isotherm	Value of parameters			
	Parameters	**25 °C**	**35 °C**	**45 °C**
Langmuir	$q_{m\ exp}$ (mg/g)	254.75	355.26	425.84
	q_m (mg/g)	256.82	359.2	428.8
	K_L (L/mg)	0.042	0.04628	0.079
	R_L	0.17	0.15	0.10
	Reduced Chi-Sqr	28.83295	49.90252	108.64149
	Residual Sum of Squares	461.32728	798.44031	1738.26384
	R-Square (COD)	0.99648	0.99658	0.99468
	Adj. R-Square	0.99626	0.99637	0.99435
	R^2	0.995	0.9961	0.9938
Freundlich	n	2.68	2.21	0.496
	K_F (mg/g) $(L/mg)^{1/n}$	41.089	46.9	67.21
	Reduced Chi-Sqr	493.17842	333.17728	280.8034
	Residual Sum of Squares	7890.85477	5330.83652	4212.05094
	R-Square (COD)	0.93972	0.97718	0.9848
	Adj. R-Square	0.93595	0.97575	0.98379
	R^2	0.936	0.9742	0.982
Dubinin–Radushkevich	$Q_{DR}(mg.g^{-1})$	232.04	301.62	354.2
	K_{DR} (mol^2/kJ^2)	2.40711E-5	1.38638E-5	4.03151E-6
	Ea (kJ/mol)	30.18	31.62	33.2
	Reduced Chi-Sqr	589.4937	1525.39951	2277.97539
	Residual Sum of Squares	9431.89916	24406.39216	36447.60617
	R-Square (COD)	0.92794	0.89552	0.88848
	Adj. R-Square	0.92344	0.88899	0.88151
	R^2	0.924	0.884	0.882
Temkin	b_T (J/mol)	39.9	29.15	24.54
	K_T (L/mol)	0.432	0.57	1.14
	Reduced Chi-Sqr	60.66051	68.56615	305.5601

	Residual Sum of Squares	970.56819	1097.05834	4888.96157
	R-Square (COD)	0.99259	0.9953	0.98504
	Adj. R-Square	0.99212	0.99501	0.98411
	R^2	0.9932	0.9952	0.985
Jossens	K	10.78	23.06	58.6
	J	0.024	0.092	0.25
	Reduced Chi-Sqr	19.16068	33.25771	43.26554
	Residual Sum of Squares	287.41026	498.86567	648.98312
	R-Square (COD)	0.9978	0.99786	0.99801
	Adj. R-Square	0.99751	0.99758	0.99775
	R^2	0.9962	0.9965	0.998

Table S8. Models of adsorption kinetic parameters of Cd(II) ions on FAACP hydrogel beads.

Model	**Value of parameters**			
	Parameters	**25 °C**	**35 °C**	**45 °C**
Pseudo-First-order kinetic	K_1 (min^{-1})x10^{-2}	0.022	0.028	0.032
	Reduced Chi-Sqr	7.90845	15.83493	22.00265
	Residual Sum of Squares	150.26052	300.86364	418.05031
	R-Square (COD)	0.99865	0.99724	0.98724
	Adj. R-Square	0.99858	0.9977	0.9776
	R^2	0.996	0.9958	0.981
Pseudo-second-order kinetic	K_2 (g.$mg^{-1}min^{-1}$)x10^{-2}	8.34168E-5	5.89495E-5	5.00099E-5
	q_e (mg/g)	255.6	358.2	422.4
	Reduced Chi-Sqr	10.03849	20.09988	27.9288
	Residual Sum of Squares	190.73137	381.89769	530.64719
	R-Square (COD)	0.99829	0.9974	0.98754
	Adj. R-Square	0.9982	0.9968	0.9868
	R^2	0.9981	0.996	0.971

Intraparticle diffusion	K_i ($mgg^{-1}min^{1/2}$)	27.38029	38.74	45.66
	X (mg/g)	2.005	2.83	3.34
	Reduced Chi-Sqr	155.19909	310.75217	431.79043
	Residual Sum of Squares	2948.78262	5904.29121	8204.01825
	R-Square (COD)	0.97352	0.9728	0.97418
	Adj. R-Square	0.97212	0.9734	0.97402
	R^2	0.973	0.982	0.974
Elovich	β (g/mg)	77.89	110.22	129.93
	α ($mgg^{-1}.min^{-1}$)	0.00358	0.00253	0.00215
	Reduced Chi-Sqr	26.32628	52.71261	73.24422
	Residual Sum of Squares	500.19939	1001.53956	1391.64017
	R-Square (COD)	0.99551	0.9962	0.9881
	Adj. R-Square	0.99527	0.9968	0.9876
	R^2	0.9948	0.997	0.9854
Experimental data	q_e (exp) (mmol/g)	253.2	361.6	425.1

Table S9. The thermodynamic parameters.

T (K)	ΔG (kJ/mol)	ΔH^o (kJ/mol)	ΔS^o (J/mol.K)
293	-0.67826		
298	-2.21302	89.25	306.95
303	-3.74778		
308	-5.28255		
313	-6.81731		
318	-8.35208		

Table S10. Characteristic of the real water samples.

Parameter	**Tap Water**	**Sea Water**	**Waste water**
pH	7.6	8.4	4.8
Total Dissolved Solids (mg/L)	384.8	22177	3564
Turbidity (NTU)	1.4	3.1	30.64
Electrical Conductivity (μS/cm)	580	33600	5400
Total Hardness (as $CaCO_3$, mg/L)	194	5850	740
Mg^{2+} (mg/L)	26	1280	136
Ca^{2+} (mg/L)	74	396	184
K^{+} (mg/L)	6.1	374	62
Cl^{-} (mg/L)	114	20600	1360
Na^{+} (mg/L)	72	9450	870
HCO_3^{-} (mg/L)	186	131	320
SO_4^{2-} (mg/L)	84	3250	614
Fe (mg/L)	0.06	0.61	3.2
Mn (mg/L)	0.05	0.08	1.4
Ni (mg/L)	0.60	0.70	2.8
Zn (mg/L)	0.16	0.12	12.4
Chemical Oxygen Demand (COD, mg/L)	20	36	845
Total Organic Carbon (TOC, mg/L)	2.84	6.2	188
Residual Chlorine (mg/L)	0.56	0.4	ND
Dominant Interfering Substances	Ca^{2+}, Mg^{2+}, HCO_3^{-}	Na^{+}, Cl^{-}, SO_4^{2-}	Zn^{2+}, Fe^{2+}, Cu^{2+}, organics
Cd(II) Removal Efficiency (%)	96.2	82.6	91.2

Table S11. Comparison of Cd(II) ions adsorption capacity in various adsorbents.

Materials	Q_e (mg/g)	Initial concentration (mg/L)	pH	Adsorbent dose (g/L)	Ref.
Canna indica-derived biochar	188.8	10–300	5	0.5	[13]
Methylisothiocyanate decorated PAMAM dendrimer/mesoporous silica	97.8	10–200	6	0.2	[14]
Cellulose/ ethylenediaminetetraacetic acid	33.2	10–150	5.5	1	[15]
Carboxymethyl cellulose/polyacrylamide	256.4	20–300	6	0.5	[16]
TiO_2/glutaraldehyde/carboxymethyl cellulose	274.28	10–300	5.5	0.5	[17]
Graphene oxide/carboxymethyl cellulose	46.13	10–200	5	0.5	[18]
Poly(vinyl alcohol)/chitosan	148	10–200	5.5	0.5	[19]
Poly(glycidyl methacrylate)/cellulose/ iminodiacetic acid	53.4	10–150	6	0.3	[20]
Chelating polyacrylonitrile	146	10–200	5.5	0.5	[21]
Polyacrylonitrile/Na-Y-zeolite/amidoxime	39.4	10–150	5	0.5	[22]
Cellulose nanocrystalline	57.76	10–200	5.5	0.5	[23]
Amidoxime chelating resin	20.7	10–100	5	0.5	[24]
Blue algae-derived biochar	135.7	10–250	5.5	0.5	[25]
Fe/Zn/*durian shells* biochar	99.83	10–200	5	0.5	[26]
Struvite/attapulgite	121.14	10–250	6	0.5	[27]
Biochar derived-sewage	127.9	20–300	5.5	0.5	[28]

sludge/calcium sulfate					
Danthron/MWCNTs	52.9	10–200	5.5	0.2	[29]
Hydroxyapatite	12.36	10–100	6	1	[30]
Ca-Mg phosphate based on dolomite	241.7	20–300	5.5	0.5	[31]
Unmodifed Cel	13.6	10–100	5	0.5	[32]
Cel/PAN/AO	123.23	10–200	5.5	0.5	[32]
FAACP Hydrogel beads	254.57	10–300	6	0.8	This wor

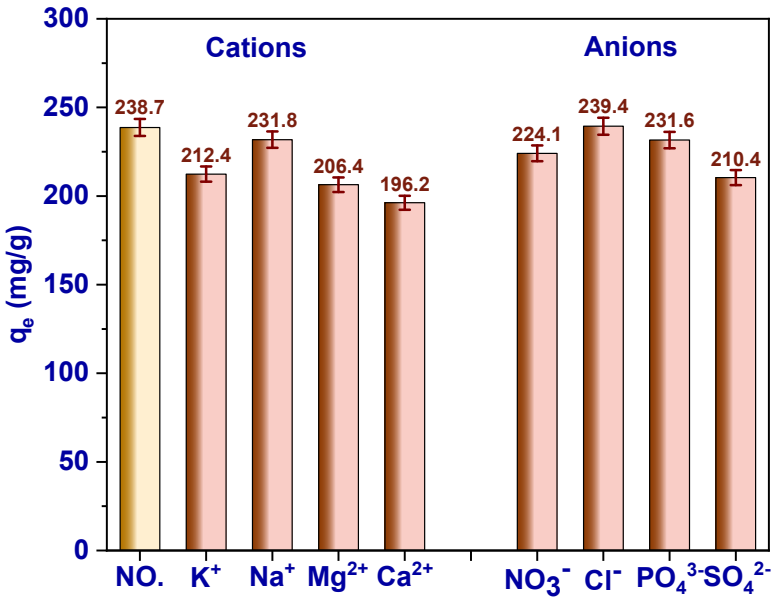

Fig. S1. Effect of interference ions.

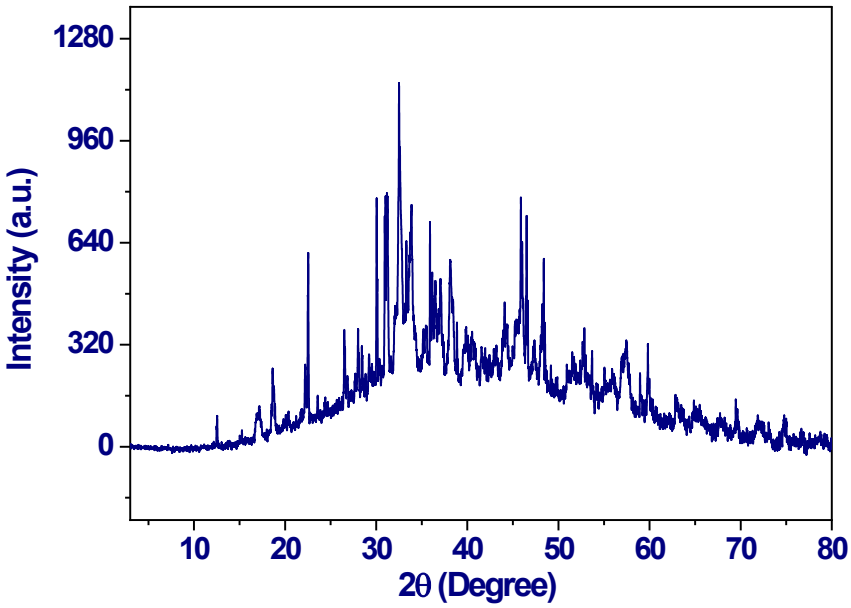

Fig. S2. XRD pattern of regenerated FAACP.

References

[1] I. Langmuir, The constitution and fundamental properties of solids and liquids. Part I. Solids, J. Am. Chem. Soc., 38 (1916) 2221-2295.
[2] H.M.F. Freundlich, Over the adsorption in solution, J. Phys. Chem., 57 (1906) 385-471.
[3] M. Dubinin, The equation of the characteristic curve of activated charcoal, Proc. Acad. Sci. USSR Phys. Chem. Sect., 55 (1947) 327-329.
[4] V.P. M.I. Tempkin, Kinetics of ammonia synthesis on promoted iron catalyst, Acta Phys. Chim. USSR, 12 (1940) 327-356.
[5] J. Bayuo, K.B. Pelig-Ba, M.A. Abukari, Isotherm modeling of lead (II) adsorption from aqueous solution using groundnut shell as a low-cost adsorbent, IOSR J Appl Chem (IOSR-JAC), 11 (2018) 18-23.
[6] S.K. Lagergren, About the theory of so-called adsorption of soluble substances, Sven. Vetenskapsakad. Handingarl, 24 (1898) 1-39.
[7] Y.-S. Ho, G. McKay, Sorption of dye from aqueous solution by peat, Chemical engineering journal, 70 (1998) 115-124.
[8] W.J. Weber Jr, J.C. Morris, Kinetics of adsorption on carbon from solution, J. Sanit. Eng. Div., 89 (1963) 31-59.

[9] M.H. Dehghani, A. Dehghan, A. Najafpoor, Removing Reactive Red 120 and 196 using chitosan/zeolite composite from aqueous solutions: Kinetics, isotherms, and process optimization, Journal of Industrial and Engineering Chemistry, 51 (2017) 185-195.
[10] E.C. Lima, A. Hosseini-Bandegharaei, J.C. Moreno-Piraján, I. Anastopoulos, A critical review of the estimation of the thermodynamic parameters on adsorption equilibria. Wrong use of equilibrium constant in the Van't Hoof equation for calculation of thermodynamic parameters of adsorption, Journal of molecular liquids, 273 (2019) 425-434.
[11] H.N. Tran, S.-J. You, A. Hosseini-Bandegharaei, H.-P. Chao, Mistakes and inconsistencies regarding adsorption of contaminants from aqueous solutions: a critical review, Water research, 120 (2017) 88-116.
[12] B. Oladipo, E. Govender-Opitz, T.V. Ojumu, Kinetics, thermodynamics, and mechanism of Cu (II) ion sorption by biogenic iron precipitate: using the lens of wastewater treatment to diagnose a typical biohydrometallurgical problem, ACS omega, 6 (2021) 27984-27993.
[13] X. Cui, S. Fang, Y. Yao, T. Li, Q. Ni, X. Yang, Z. He, Potential mechanisms of cadmium removal from aqueous solution by Canna indica derived biochar, Science of the Total Environment, 562 (2016) 517-525.
[14] L. Luan, B. Tang, Y. Liu, W. Xu, Y. Liu, A. Wang, Y. Niu, Direct synthesis of sulfur-decorating PAMAM dendrimer/mesoporous silica for enhanced Hg (II) and Cd (II) adsorption, Langmuir, 38 (2022) 698-710.
[15] A. Daochalermwong, N. Chanka, K. Songsrirote, P. Dittanet, C. Niamnuy, A. Seubsai, Removal of heavy metal ions using modified celluloses prepared from pineapple leaf fiber, ACS omega, 5 (2020) 5285-5296.
[16] C.B. Godiya, X. Cheng, D. Li, Z. Chen, X. Lu, Carboxymethyl cellulose/polyacrylamide composite hydrogel for cascaded treatment/reuse of heavy metal ions in wastewater, Journal of hazardous materials, 364 (2019) 28-38.
[17] M.E. Mahmoud, A.E. Abdou, M.E. Sobhy, N.A. Fekry, Solid–solid crosslinking of carboxymethyl cellulose nanolayer on titanium oxide nanoparticles as a novel biocomposite for efficient removal of toxic heavy metals from water, International journal of biological macromolecules, 105 (2017) 1269-1278.
[18] Y. Zhang, Y. Liu, X. Wang, Z. Sun, J. Ma, T. Wu, F. Xing, J. Gao, Porous graphene oxide/carboxymethyl cellulose monoliths, with high metal ion adsorption, Carbohydrate polymers, 101 (2014) 392-400.
[19] M.R. Karim, M.O. Aijaz, N.H. Alharth, H.F. Alharbi, F.S. Al-Mubaddel, M.R. Awual, Composite nanofibers membranes of poly (vinyl alcohol)/chitosan for selective lead (II) and cadmium (II) ions removal from wastewater, Ecotoxicology and environmental safety, 169 (2019) 479-486.
[20] M. Barsbay, P.A. Kavaklı, S. Tilki, C. Kavaklı, O. Güven, Porous cellulosic adsorbent for the removal of Cd (II), Pb (II) and Cu (II) ions from aqueous media, Radiation Physics and Chemistry, 142 (2018) 70-76.
[21] P. Bhunia, S. Chatterjee, P. Rudra, S. De, Chelating polyacrylonitrile beads for removal of lead and cadmium from wastewater, Separation and Purification Technology, 193 (2018) 202-213.
[22] K. Elwakeel, A. El-Bindary, E. Kouta, E. Guibal, Functionalization of polyacrylonitrile/Na-Y-zeolite composite with amidoxime groups for the sorption of Cu (II), Cd (II) and Pb (II) metal ions, Chemical Engineering Journal, 332 (2018) 727-736.
[23] H.T. Kara, S.T. Anshebo, F.K. Sabir, Adsorptive removal of Cd (II) ions from wastewater using maleic anhydride nanocellulose, Journal of Nanotechnology, 2021 (2021) 9966811.
[24] C. Zheng, C. He, Y. Yang, T. Fujita, G. Wang, W. Yang, Characterization of waste amidoxime chelating resin and its reutilization performance in adsorption of Pb (II), Cu (II), Cd (II) and Zn (II) Ions, Metals, 12 (2022) 149.
[25] P. Liu, D. Rao, L. Zou, Y. Teng, H. Yu, Capacity and potential mechanisms of Cd (II) adsorption from aqueous solution by blue algae-derived biochars, Science of the Total Environment, 767 (2021) 145447.

[26] T. Yang, Y. Xu, Q. Huang, Y. Sun, X. Liang, L. Wang, X. Qin, L. Zhao, Adsorption characteristics and the removal mechanism of two novel Fe-Zn composite modified biochar for Cd (II) in water, Bioresource technology, 333 (2021) 125078.
[27] H. Wang, X. Wang, J. Ma, P. Xia, J. Zhao, Removal of cadmium (II) from aqueous solution: a comparative study of raw attapulgite clay and a reusable waste–struvite/attapulgite obtained from nutrient-rich wastewater, Journal of hazardous materials, 329 (2017) 66-76.
[28] L. Liu, T. Yue, R. Liu, H. Lin, D. Wang, B. Li, Efficient absorptive removal of Cd (Ⅱ) in aqueous solution by biochar derived from sewage sludge and calcium sulfate, Bioresource Technology, 336 (2021) 125333.
[29] T. Shahryari, P. Singh, P. Raizada, A. Davidyants, L. Thangavelu, S. Sivamani, A. Naseri, F. Vahidipour, A. Ivanets, A. Hosseini-Bandegharaei, Adsorption properties of Danthron-impregnated carbon nanotubes and their usage for solid phase extraction of heavy metal ions, Colloids and surfaces A: physicochemical and engineering aspects, 641 (2022) 128528.
[30] A. Ivanets, N. Kitikova, I. Shashkova, M.Y. Roshchina, V. Srivastava, M. Sillanpää, Adsorption performance of hydroxyapatite with different crystalline and porous structure towards metal ions in multicomponent solution, Journal of Water Process Engineering, 32 (2019) 100963.
[31] A. Ivanets, V. Srivastava, N. Kitikova, I. Shashkova, M. Sillanpää, Non-apatite Ca-Mg phosphate sorbent for removal of toxic metal ions from aqueous solutions, Journal of environmental chemical engineering, 5 (2017) 2010-2017.
[32] H.A. Abdelmonem, T.F. Hassanein, H.E. Sharafeldin, H. Gomaa, A.S. Ahmed, A.M. Abdel-lateef, E.M. Allam, M.F. Cheira, M.E. Eissa, A.H. Tilp, Cellulose-embedded polyacrylonitrile/amidoxime for the removal of cadmium (II) from wastewater: Adsorption performance and proposed mechanism, Colloids and Surfaces A: Physicochemical and Engineering Aspects, 684 (2024) 133081.